Correction

APPLIED BIOLOGICAL SCIENCES, ENGINEERING

Correction for "Dendrimer-RNA nanoparticles generate protective immunity against lethal Ebola, H1N1 influenza, and *Toxoplasma gondii* challenges with a single dose," by Jasdave S. Chahal, Omar F. Khan, Christopher L. Cooper, Justine S. McPartlan, Jonathan K. Tsosie, Lucas D. Tilley, Saima M. Sidik, Sebastian Lourido, Robert Langer, Sina Bavari, Hidde L. Ploegh, and Daniel G. Anderson, which appeared in issue 29, July 19, 2016, of *Proc Natl Acad Sci USA* (113:E4133–E4142; first published July 5, 2016; 10.1073/pnas.1600299113).

The authors note that a statement in the Acknowledgments appeared incorrectly. "Partial support was provided by Medi-Vector, Inc. Grant OSP 30-1765-9901" should instead appear as "Partial support was provided by Fujifilm/MediVector, Inc. Grant OSP 30-1765-9901."

PNAS

Dendrimer-RNA nanoparticles generate protective immunity against lethal Ebola, H1N1 influenza, and *Toxoplasma gondii* challenges with a single dose

Jasdave S. Chahal[a,1], Omar F. Khan[b,1], Christopher L. Cooper[c], Justine S. McPartlan[a], Jonathan K. Tsosie[b], Lucas D. Tilley[a], Saima M. Sidik[a], Sebastian Lourido[a], Robert Langer[b,d,e,f,g], Sina Bavari[c], Hidde L. Ploegh[a], and Daniel G. Anderson[b,c,d,f,g,2]

[a]Whitehead Institute for Biomedical Research, Cambridge, MA 02142; [b]David H. Koch Institute for Integrative Cancer Research, Massachusetts Institute of Technology, Cambridge, MA 02139; [c]Molecular and Translational Sciences, United States Army Medical Research Institute of Infectious Diseases, Fort Detrick, MD 21702; [d]Department of Biology, Massachusetts Institute of Technology, Cambridge, MA 02139; [e]Department of Chemical Engineering, Massachusetts Institute of Technology, Cambridge, MA 02139; [f]Institute for Medical Engineering and Science, Massachusetts Institute of Technology, Cambridge, MA 02139; and [g]Harvard-MIT Division of Health Science and Technology, Massachusetts Institute of Technology, Cambridge, MA 02139

Vaccines have had broad medical impact, but existing vaccine technologies and production methods are limited in their ability to respond rapidly to evolving and emerging pathogens, or sudden outbreaks. Here, we develop a rapid-response, fully synthetic, single-dose, adjuvant-free dendrimer nanoparticle vaccine platform wherein antigens are encoded by encapsulated mRNA replicons. To our knowledge, this system is the first capable of generating protective immunity against a broad spectrum of lethal pathogen challenges, including H1N1 influenza, *Toxoplasma gondii*, and Ebola virus. The vaccine can be formed with multiple antigen-expressing replicons, and is capable of eliciting both CD8+ T-cell and antibody responses. The ability to generate viable, contaminant-free vaccines within days, to single or multiple antigens, may have broad utility for a range of diseases.

nanoparticle | vaccine platform | replicon | viruses | parasites

Today, there are a range of vaccine technologies used clinically, with varied use of inactivated pathogens, molecular antigens, adjuvants, delivery technologies, administration routes, and dosing regimes (1–13). Although existing vaccine systems have had a huge impact on prevention of infectious disease, challenges remain. There is a need for safe and effective vaccines that are flexible—capable of rapid, on-demand production and optimization near the point of care (14, 15).

As one of the standard vaccine forms, live-attenuated vaccines can confer long-lasting immunity, in part, due to their ability to undergo limited replication in the host. Such vaccines mimic natural infection and drive endogenous antigen production and presentation by host class I major histocompatibility complex (MHC) molecules (16). However, safety issues (e.g., reversion to virulence, contamination due to production in living systems) and manufacturing limitations [e.g., long times necessary for growth in eggs or cell culture, poor shelf-life (17)] complicate the development and production of live vaccines. Recombinant subunit vaccines, which consist of single or multiple protein antigens produced in bacteria, yeast, or plants, can be synthesized more rapidly and do not pose the risk of reversion or genotoxicity, but they are often less immunogenic. In addition, cell-based production necessitates extensive purification steps, hampering efforts to respond to outbreaks rapidly. DNA-based vectors used for gene-based vaccination (18–20) have shown efficacy in humans (21), but raise safety concerns due to the risk of mutagenic integration into the patient's genome (22, 23). Nonretroviral RNA vaccines are attractive due to their inherent transience and absence of recombination or integration into the patient's genome. However, RNA-based vaccines require intracellular delivery methods to function (24–29).

Replicon mRNA, a type of self-replicating nucleic acid, can substantially amplify the production of encoded protein, leading to sustained translation (30). This ability to produce large amounts of antigen and self-adjuvant through replication via dsRNA intermediates has motivated investigation into their potential as a vaccine (31). However, delivery is required for replicon mRNA function, and, to date, there has been no report of protective immunity capable of allowing for survival against a lethal challenge of any pathogen using nonviral, fully synthetic approaches (32). Naked replicon mRNA can activate the innate immune system upon administration, which can limit translational efficiency, diminish potency, and induce toxicity (33–36). RNA, particularly single-stranded RNA, is rapidly degraded by nucleases when injected in vivo (37). Although therapeutic RNA can be chemically modified to facilitate delivery and reduce immunogenicity (38–41), no such modifications have been reported for replicons; this may reflect the sensitivity of the viral replicase to base modification (42–44) or to the secondary structure effects modifications may have on vital conserved RNA replication elements (45). We reasoned that nanoformulation could allow for the protection and functional delivery of replicon mRNA vaccines.

Significance

To respond better to evolving pathogens, sudden outbreaks, and individual patient needs, a flexible, safe, and efficient vaccine platform amenable to rapid production near the point of care is required. To this end, we created a fully synthetic, single-dose, adjuvant-free nanoparticle vaccine platform wherein modified dendrimer molecules nanoencapsulate antigen-expressing replicon mRNAs. Vaccines can be multiplexed and formed with multiple antigen-expressing replicons. After a single immunization, the rapid-production, contaminant-free vaccines elicit vital CD8+ T-cell and antibody responses that fully protect against lethal exposures to several deadly pathogens, including Ebola virus, H1N1 influenza, and *Toxoplasma gondii*. We believe this technology may allow for rapid-response vaccines with broad efficacy that reduce the number and frequency of vaccinations, and healthcare worker burden.
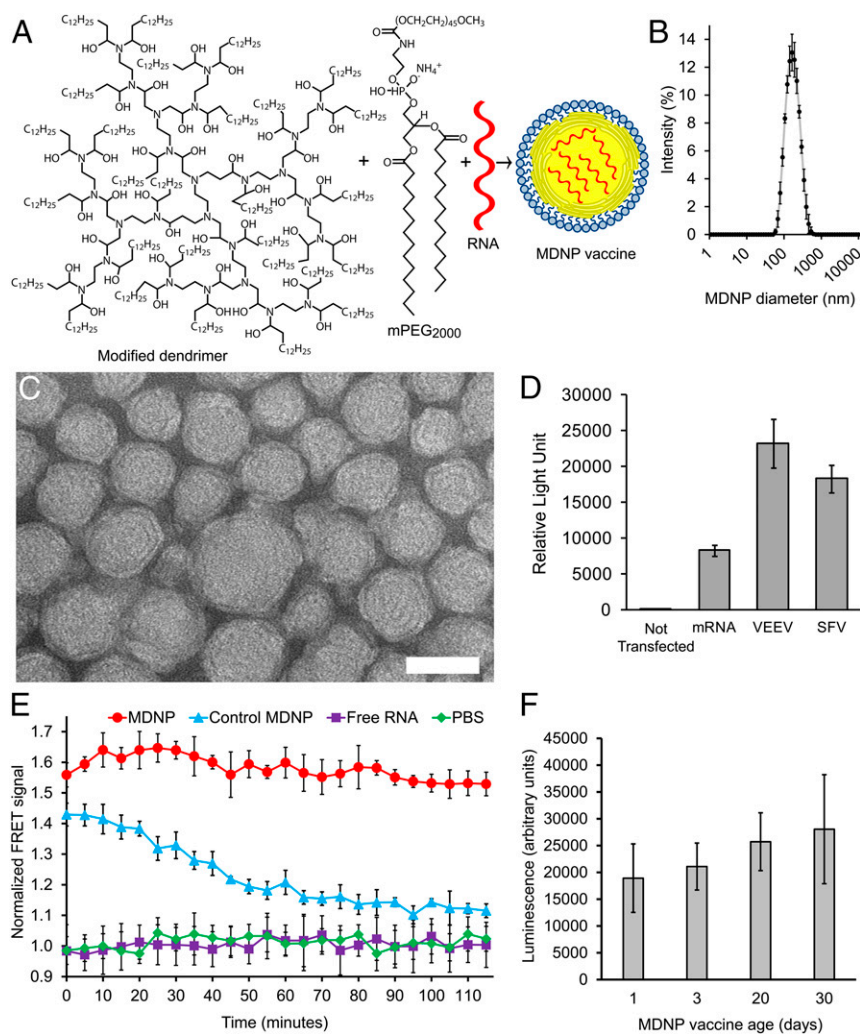
Fig. 1. MDNP vaccine platform. (*A*) Ionizable dendrimer-based nanomaterial, a lipid-anchored PEG, and RNA are combined to form the final vaccine nanoparticle. Additional characterization is provided in Fig. S9. (*B*) Size distribution of the MDNPs by dynamic light scattering. Error bars ± SD and *n* = 3. (*C*) Transmission electron micrograph of MDNPs. (Scale bar: 50 nm.) (*D*) Firefly luciferase activity in BHK cells mediated by conventional mRNA and replicon RNAs based on VEEV and SFV genomes, assayed 14 h posttransfection. Error bars ± SD and *n* = 3. (*E*) Stability of formulated nanoparticles using different nanomaterials over 2 h in 50% AB human serum at 37 °C. MDNPs were formulated to contain an equimolar mixture of RNAs labeled with Alexa Fluor 594 and Alexa Fluor 647. When in close contact (i.e., within the intact MNDP), the RNAs would act as a FRET pair. When the MDNPs disassembled, the released RNAs would no longer close enough to generate a FRET signal. To measure FRET, the samples were excited at 540 nm and the fluorescence intensity was read at 690 and 620 nm. FRET was determined as the ratio of the fluorescence intensities at 690/620 nm. FRET signals were normalized to the signals of free RNA controls. The more stable MDNP nanomaterial was synthesized using 2-tridecyloxirane, whereas the less stable control MDNP used 1,2-Epoxydodecane. Negative controls were free RNA. PBS was used to determine background levels. The FRET signal was normalized to the value of the completely ruptured nanoparticles. Nanoencapsulation in the MDNP provides superior protection because nanoparticles remain intact and do not release their RNA payloads while in whole human serum. Because of this stability, the RNA payloads are protected from endonuclease degradation. Error bars ± SD and *n* = 4–8. (*F*) Vaccine stability over long periods of storage. Nanoparticles containing luciferase replicon RNA were created and stored at 4 °C for extended periods of time. HeLa cells were treated with a fixed amount of the nanoparticles, and luciferase expression was assayed after 14 h. After a minimum of 30 d of storage, no statistically significant changes in luciferase transfection efficiency were detected by ANOVA analysis (with Tukey multiple comparison correction), indicating the particles remained stable and the RNA payload remained intact. Error bars ± SD and *n* = 4.

Cationic and ionizable materials have shown promise as nanoparticulate nucleic acid delivery systems (46). Given the very large size of replicon mRNA, and lack of chemical modification necessary for mRNA replicon function, we reasoned that charge-dense polyamines might provide optimal protection from nucleases in the body while allowing for functional release in the cytoplasm. Charge-dense polyamines, such as those polyamines based on polyethylene imine, can condense nucleic acids through interaction with the phosphate backbone, resulting in compact nanoparticles that provide a measure of protection against nucleases (46). Furthermore, these materials often contain amines with pK_a values between 5 and 7, which have been observed to facilitate release of endocytosed nucleic acid into the cytoplasm (47–50). We further reasoned that the use of monodisperse, molecularly defined dendrimers instead of more polydisperse amine polymers would allow for better definition of nanoparticulate composition following self-assembly, and reduce efforts needed to confirm the identity and batch-to-batch reproducibility of these often heterogeneous materials (51). Here, we develop dendrimer formulations with self-replicating RNA to deliver antigenic RNA payloads in vivo, resulting in antibody production and antigen-specific CD8^{+} T-cell responses against the encoded protein antigen, as well as protective immunity and survival to lethal pathogen challenges.

Conventional unmodified in vitro-transcribed mRNA, and replicon RNAs based on the genomes of two alphaviruses, Venezuelan equine encephalitis virus (VEEV) and Semliki Forest virus
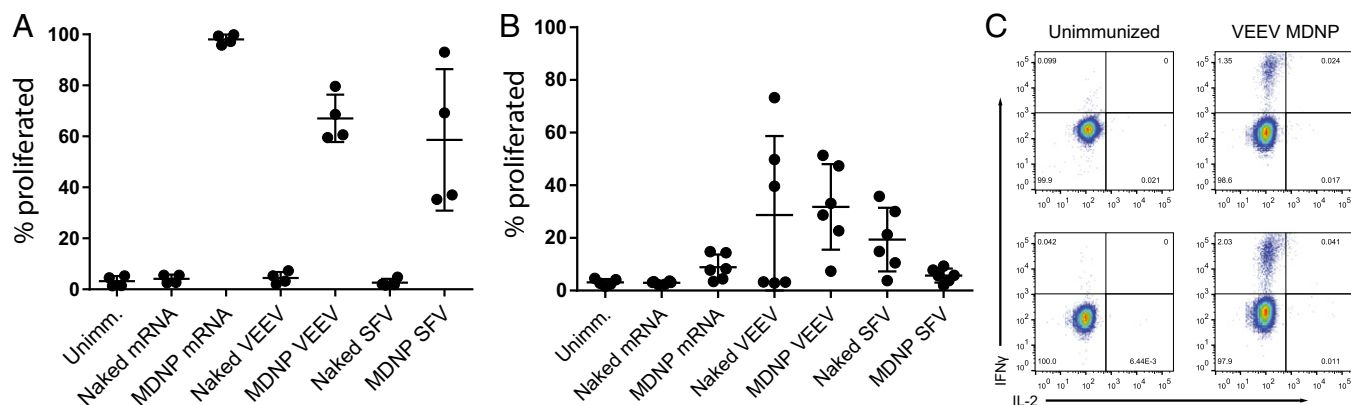
Fig. 2. MDNP RNA vaccines stimulate CD8^{+} T-cell responses against a model intracellular antigen. (*A*) Quantification of four independent biological replicates of OT-1 proliferation assay performed 4 d posttransfer/3 d postimmunization. Error bars ± SD. (*B*) Quantification of six independent biological replicates of OT-1 proliferation assay performed 10 d posttransfer/14 d postimmunization. Error bars ± SD. (*C*) Intracellular cytokine staining for IFN-γ and IL-2 on splenocytes of VEEV-cOVA MDNP-immunized mice 9 d postinjection, gated on CD8^{+} cells. Independent results are shown for two unimmunized (*Left*) and two immunized (*Right*) mice. Unimm., unimmunized.

(SFV), were developed that support self-amplification via an immunogenic double-stranded RNA intermediate in the cytoplasm to drive efficient antigen expression. We show that a modified dendrimer nanoparticle (MDNP)-delivered VEEV replicon RNA encoding the hemagglutinin protein (HA) of an H1N1 influenza virus (A/WSN/33) or the Ebola virus (EBOV) glycoprotein (GP) protects mice against lethal viral infection. A multiplexed MDNP vaccine that simultaneously carries multiple replicons encoding dense granule protein 6 (GRA6), rhoptry protein 2A (ROP2A), rhoptry protein 18 (ROP18), surface antigen 1 (SAG1), surface antigen 2A (SAG2A), and apical membrane antigen 1 (AMA1) also protects mice against lethal *Toxoplasma gondii* challenges. Thus, this platform is capable of generating protection against representative diseases from all three categories of the National Institute of Allergy and Infectious Diseases' Priority Pathogen List for emerging and rapidly increasing threats (52). Importantly, generation of a new MDNP vaccine system composed of these dendrimers and replicon RNA takes only about 1 wk, in contrast to the cell culture and fertilized egg systems that can take 6 mo or more to develop (53–58). In addition, postproduction purification required for this MDNP system is minimal, as is the risk of contaminating allergens relative to existing vaccine systems (59–61). Finally, this synthetic system is able to produce multiple antigens and to induce appropriate antibody and T-cell responses without additional adjuvants in a range of disease models. We believe the delivery technology developed here may serve as a flexible, scalable, and potent approach to immunization.

Results

MDNPs Protect RNA Payloads and Are Stable. Nanoparticle-based vaccines should elicit robust antigen expression, protect the RNA payload from environmental RNase activity, and preserve these properties during storage. To test whether our MDNP (Fig. 1 *A–C*) exhibited these characteristics, a VEEV replicon RNA encoding firefly luciferase was selected as a model nanoencapsulation cargo. Low polydispersity particles (Fig. 1 *B* and *C*) were routinely produced using this method. We chose this payload because VEEV-driven luciferase expression in tissue culture was the strongest of the three RNA types tested (conventional mRNA, VEEV replicon, and SFV replicon) (Fig. 1*D*). The VEEV replicon RNA was formulated into MDNPs using a microfluidic-based production method (49, 50).

The nanomaterial's ability to generate RNA-containing nanoparticles that remain stable while in human serum was verified by fluorescence resonance energy transfer (FRET) assay (62) (Fig. 1*E*). To confirm long-term stability, HeLa cells were treated with MDNPs containing luciferase-expressing replicons, which had been

stored following formulation for varying times. No statistically significant changes in luminescence were observed when using particles stored at 4 °C for 1, 3, 22, or 30 d (Fig. 1*F*).

The modified dendrimer is fully synthetic and purified, and the RNA payload is produced in the complete absence of cells. The MDNP nanomaterial has been established not to cause systemic increases in inflammatory cytokines in vivo at doses an order of magnitude greater than used for the immunizations described in this report (49, 50). The particle preparations used in these studies are free of infectious contaminants and virtually endotoxin-free [<0.228 endotoxin units per milliliter, which is 40-fold lower than an acceptable endotoxin burden for viral/nonviral vectors (63)].

RNAs Nanoencapsulated in MDNPs Drive Expression at the Site of Intramuscular Injection and Stimulate Antigen-Specific T Cells in Vivo. The MDNP-encapsulated RNAs were successfully expressed in a broad variety of cell types in culture, including the human epithelial cell line HeLa, murine and human primary fibroblasts, the mouse dendritic cell line DC2.4, the murine and rat skeletal myoblast cell lines C2C12 and L6, and differentiated mouse myotubes derived from the C2C12 cell line (Fig. S1*A* and Table S1). Intramuscular injection of MDNP was observed to drive readily detectible gene expression at the site of injection in vivo (Fig. S1*B*). To test whether or not an immune response was induced using the MDNP system, a cytoplasmically expressed ovalbumin fragment (cOVA) (64) was used as a model intracellular antigen. We produced conventional mRNA, VEEV replicon RNAs, and SFV replicon RNAs to express this protein. The cOVA protein contains the dominant epitope recognized by CD8^{+} T cells (64). The expression of cOVA 14 h posttransfection in BHK21 cells was confirmed by immunoblot analysis, with the VEEV replicon proving to be the most robust (Fig. S2*A*). To determine if antigen expression was sufficient to activate CD8^{+} T cells in vivo using MDNPs, transgenic mice exclusively expressing a T-cell receptor (TCR) specific for the immunodominant H-2K$_b$–restricted ovalbumin epitope SIINFEKL (OT-1 transgenic/Rag1-knockout mice) were used as lymphocyte donors in an adoptive transfer experiment. Mice that received OT-1 T cells were given either unpackaged ("naked") RNA or the same RNA encapsulated as MDNPs by bilateral intramuscular leg injection. Three days postimmunization, OT-1 T-cell proliferation was determined by 5-(and 6-)Carboxyfluorescein diacetate succinimidyl ester (CFSE) dilution (Fig. 2*A* and Fig. S2*B*). Mice immunized with naked RNA showed no OT-1 cell proliferation. In contrast, at least six rounds of proliferation were detected in mice that received RNAs as MDNPs.
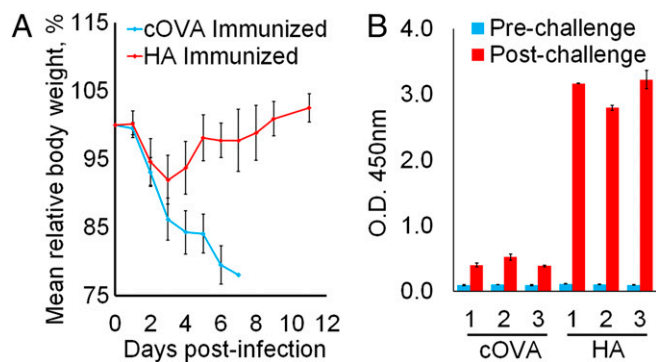
Fig. 3. Single-dose VEEV-based MDNP immunization protects against lethal H1N1 influenza challenge. (*A*) Protection against influenza challenge. Mice were infected with a lethal dose of influenza A/NWS/33 on day 0, and body weight was plotted as a percentage of preinfection weight. Mice were euthanized when body weight dropped below 80%. One hundred percent of control-immunized mice died, and 100% of HA-immunized mice fully recovered and survived for 3 wk with no signs of infection, at which point the experiment was terminated. Error bars ± SD and *n* = 3. (*B*) Serum anti-HA IgG in response to infection. HA-immunized surviving mice exhibited higher HA-specific antibody titers 7 d postinfection than control-immunized mice at the time of death. Results for each individual animal are shown. Error bars ± SD of technical duplicates.

The strongest proliferation was observed in mice immunized with nonreplicon conventional mRNA MDNPs. Because the doses given were based on equivalent masses of injected RNA, an ~10-fold molar excess of the conventional mRNA was injected relative to the replicon RNAs. A 10-fold higher dose of packaged VEEV replicon RNA indeed yielded a profile of OT-1 proliferation similar to dendrimer-packaged mRNA (Fig. S2*C*).

To address whether a single dose of MDNP-delivered RNAs resulted in antigen presentation over a longer period (29), C57BL/6 mice were immunized with naked or MDNP RNAs, followed by adoptive transfer of CFSE-labeled OT-1 cells 10 d later. Four days posttransfer, proliferation was analyzed (Fig. 2*B*). Naked mRNA immunization failed to induce OT-1 T-cell proliferation. Immunization with MDNP mRNAs resulted in low, but detectable, OT-1 proliferation in some mice. Immunization with naked replicon RNAs caused highly variable proliferation of OT-1 T cells. However, with the MDNP system, the VEEV replicon RNA led to consistent proliferation of OT-1 T cells in the majority of immunized mice (ranging from 20–50% proliferation in five of the six animals). MDNP-delivered SFV replicon RNA failed to induce OT-1 proliferation at this time point. VEEV superiority was further confirmed with the viral structural polyproteins HIV1 Gag (Fig. S3) and Ebola GP (Fig. S4*A*).

We therefore pursued MDNP-delivered VEEV replicons as the vaccine candidate. To confirm that VEEV MDNP could stimulate endogenous T-cell responses, C57BL/6 mice were immunized with a high 40-μg dose of cOVA VEEV MDNP. After 9 d, we measured intracellular IFN-γ and IL-2 production in splenocytes stimulated in vitro with the immunodominant H2-K^b class I MHC-restricted OVA peptide SIINFEKL (65). In two independent experiments, >1% of endogenous CD8$^+$ splenocytes from immunized mice contained discrete populations of strongly IFN-γ$^+$ cells upon peptide stimulation (Fig. 2*C*). Eighteen days postimmunization, abundant circulating CD8$^+$ T cells with TCR specificity for MHC class I-bound SIINFEKL, as detected by tetramer staining, were observed in similarly immunized mice (Fig. S5*A*). For comparison, in similar independent experiments using mRNA as the payload, fewer circulating tetramer-positive cells were detected over the course of the study, and levels were nearly undetectable by day 16 (Fig. S5*B*). These observations, coupled with the fact that alphavirus replicons induce potent type I IFN responses (66, 67) (Fig. S6), as well as apoptosis and antigen uptake by dendritic cells (68, 69), further

justified the selection of VEEV as the candidate payload for further experiments with a variety of target antigens. It should be noted that in MDNP VEEV-immunized animals, antigen-coding RNA was detectable by day 11 in the draining inguinal lymph nodes (Fig. S5*C*), raising the possibility that the immunogenic action of replicons delivered by MDNPs may not be limited to the site of injection, although the injection site is likely to be the major source of actual antigen production in vivo.

Single-Dose HA-Expressing MDNP Vaccine Protects Against Lethal Influenza Challenge. To determine whether the nanoparticle-based vaccine could elicit immunity that protects against a lethal viral challenge, RNAs encoding the influenza A/WSN/33 HA protein (Fig. S7*A*) were synthesized. HA was detected by immunoblot only when expressed from the VEEV replicon. Correct processing and shuttling of the VEEV RNA-expressed HA protein to the cell surface were confirmed by surface immunostaining with an HA-specific single-chain antibody (70) (Fig. S7*B*).

BALB/c mice were immunized with VEEV MDNPs encoding either the HA protein or an irrelevant antigen (cOVA) as a control, and challenged 14 d later with a lethal dose of influenza A/WSN/33. Control mice succumbed to infection by day 7, whereas all HA-expressing nanoparticle-immunized mice survived the challenge, and showed complete recovery of body weight by day 11 (Fig. 3*A*), with no clinical signs of infection after 3 wk. No anti-HA IgG was detected in the sera of mice 7 d postimmunization or in control mice at the time of sacrifice (6 or 7 d postinfection; Fig. 3*B*). At 7 d postchallenge, HA-reactive IgG was readily detectable in the surviving mice immunized with HA-encoding VEEV replicon MDNPs (Fig. 3*B*).

VEEV MDNP Vaccine Protects Mice from Lethal EBOV Challenge. To demonstrate the MDNP platform's versatility, an EBOV vaccine was created. Although no licensed US Food and Drug Administration vaccine for EBOV is currently available, most existing EBOV vaccine platforms center on the viral GP as the primary target antigen. Therefore, RNAs expressing full-length Kikwit EBOV GP were synthesized. As was observed for influenza HA, GP expression was difficult to detect in lysates from all but the VEEV replicon-transfected cells. We could not detect GP in cells transfected with conventional unstabilized mRNA, but we observed a weak signal in cells transfected with 3′ UTR-stabilized mRNA or SFV replicon RNA (Fig. S4*A*). Based on the EBOV GP expression profile, the VEEV replicon was used as the MDNP payload (Fig. S4*B*).

Mice immunized with 40 μg of VEEV-GP MDNP exhibited robust GP-specific T-cell responses 9 d after immunization, as determined by IFN-γ and IL-2 expression by CD8$^+$ and CD4$^+$ splenocytes in response to ex vivo treatment with the EBOV GP-derived WE15 peptide (71) (Fig. 4*A*). Using a prime-boost schedule of day 0 and day 21, mice were vaccinated with VEEV-GP MDNPs, naked VEEV-GP, or VEEV-cOVA MDNP, and then tested for GP-specific antibody responses. An additional group receiving a single (prime-only) injection of VEEV-GP MDNP was also tested. VEEV-GP MDNP vaccination resulted in a robust and dose-dependent humoral response, with the highest tested dose (40 μg) resulting in ~4- to 5-log titers of GP-specific IgG responses from both single-dose (prime-only) and two-dose (prime-boost) vaccinations (Fig. 4*B*). However, both antibody titers and the number of animals with detectable GP antibodies began to decline at vaccine doses below 4.0 μg.

MDNPs also protected mice against EBOV. Twenty-eight days postvaccination, animals were challenged with a lethal dose of mouse-adapted EBOV (ma-EBOV) (72). Although all control animals succumbed to EBOV infection by day 7, 100% protection was conferred by 4.0-μg and 40-μg Ebola MDNP prime-boost vaccinations, with no EBOV clinical pathological findings observed over the course of the study (Fig. 4*C*). A single high-dose MDNP prime
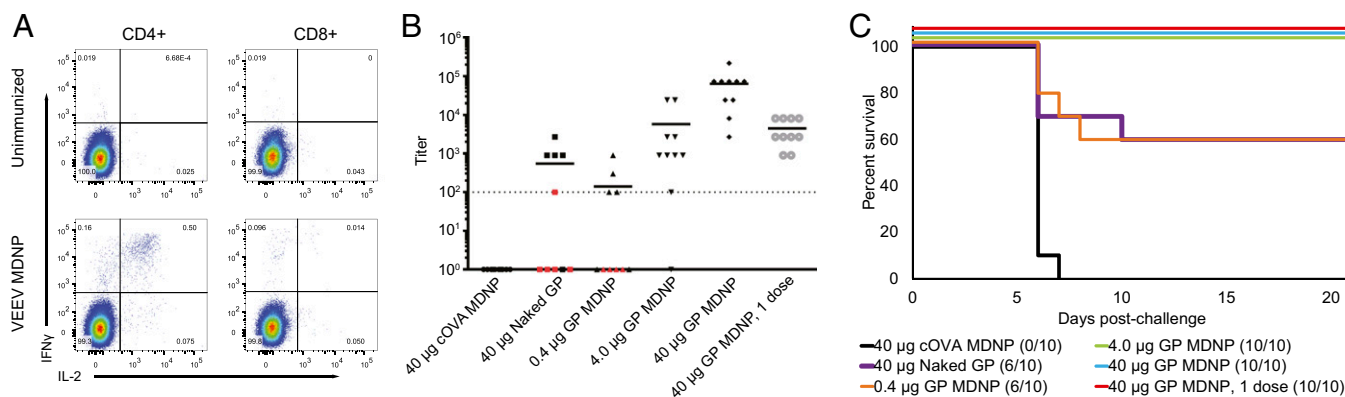
Fig. 4. VEEV-based MDNP immunization protects against lethal EBOV challenge. (*A*) EBOV-GP–specific T-cell responses assayed 9 d postimmunization with 40 μg of VEEV-GP MDNP vaccine. Splenocytes were cultured ex vivo for 6 h in the absence or presence of the EBOV-GP–derived WE15 peptide, and IFN-γ and IL-2 expression in CD8^{+} and CD4^{+} cells was assayed by intracellular cytokine staining and FACS. One representative result of three similar independent experiments is shown. (*B*) EBOV-GP specific IgG antibody titers were determined by ELISA from mice vaccinated with the indicated amounts of Ebola-GP MDNP, 40 μg of cOVA MDNP, or 40 μg of naked VEE-GP on days 0 and 21. A single-dose, prime-only vaccination with 40 μg of EBOV-GP MDNP was also tested. Titers were determined by reciprocal end-point dilution on serum from day 23 postvaccination. Red symbols denote animals that succumbed to EBOV disease. The dashed line represents the assay's level of detection. (*C*) Survival of animals following challenge with 1,000 pfu of mouse-adapted EBOV 28 d postvaccination. Control animals are denoted by a solid gray line. Study was concluded 21 d postinfection (*n* = 10 animals per group).

vaccination likewise resulted in 100% protection against lethal EBOV infection. In agreement with humoral immune responses, protection began to decrease at MDNP vaccine doses below 4.0 μg, with 60% of the animals surviving following vaccination with 0.4 μg of MDNP. Noteworthy and demonstrative of enhanced efficacy granted by MDNP nanoencapsulation, 40 μg of naked VEEV-GP and 0.4 μg of VEEV-GP MDNP elicited comparable humoral and protective responses, despite an approximate 100-fold reduction in the total amount of VEEV replicon present during vaccination. As observed with other EBOV vaccine platforms, the antibody response did not completely correlate with protection (71).

VEEV MDNP Vaccine Protects Mice Against Lethal *T. gondii* Challenge.
As a demonstration of the MDNP's large-payload capacity, a hexaplex vaccine was produced for *T. gondii*. *T. gondii* is an apicomplexan protozoan that infects one-third of world's population through contaminated food, can cause cerebral toxoplasmosis in immunocompromised individuals, and has no approved human vaccine despite efforts to generate immunity through injection of live-attenuated parasites, DNA, and peptides (73). The annual cost of this illness in the United States is estimated to be $3 billion (74). After confirming the ability to express multiple replicons simultaneously coformulated into a single MDNP (Fig. S8*A*), a multiplexed *T. gondii* MDNP vaccine was produced. Six *T. gondii*-specific antigens (GRA6, ROP2A, ROP18, SAG1, SAG2A, and AMA1) were encoded into VEEV replicons (Fig. S8*B*), and equimolar amounts were coformulated into MDNPs. These antigens were selected because they represent proteins expressed in multiple life-cycle stages of the parasite and are conserved across multiple strains and types. Animals were vaccinated with a single 40-μg dose of vaccine (6.67 μg per replicon, which is within the effective dose range established for Ebola in Fig. 4 *B* and *C*). As a control, animals were treated with a matching dose of MDNPs carrying VEEV HA as an irrelevant antigen. Thirty-two days postimmunization, animals were challenged with lethal doses of the *T. gondii* type II strain Prugniaud (PRU) (Fig. 5). By day 12, all control animals succumbed to infection. The remaining animals vaccinated with the hexaplex MDNP vaccine survived for over 6 mo with no clinical indications. To our knowledge, this is the first demonstration of a fully protective, single-dose mRNA replicon nanoparticle vaccine for *T. gondii*.

Discussion

Gene-based approaches to vaccines have a number of potential advantages over conventional methods, because they are fully synthetic and rapidly customizable, and can be produced in adjuvant-free preparations (75). Current virus-based vaccine production methods are time-consuming; they require over 5 mo of lead time, and output can be complicated by scale-up and yield issues, as experienced in the 2009 H1N1 pandemic (53). Vaccines based on gene delivery by viral vectors such as adenovirus, recombinant vesicular stomatitis virus (rVSV), adeno-associated virus (AAV), or CMV face the additional challenge of preexisting or induced antivector immunity, which precludes repeated administration. The MDNP platform can better respond to sudden outbreaks, evolving pathogens, and individual patient needs due to its flexibility, safety, and efficiency. With this platform, the time line of production from initial access to the relevant DNA sequences to milligram-scale, injection-ready MDNP vaccine is only 7 d. By facilitating replicon delivery to the cytosol, the MDNPs drive endogenous antigen production that stimulates both T-cell and antibody responses. Furthermore, because nanoencapsulation is RNA sequence-independent, a variety of different replicons, each encoding a unique antigen, can be created and coencapsulated (Fig. 5 and Fig. S8*A*). The attainable doses (up to at least 40 μg) are an order of magnitude greater than those doses needed to achieve significant protective immunity (Figs. 4 and 5). Assuming this range of therapeutic index translates to humans, we believe there is the potential to incorporate multiple distinct antigens into a single formulation.

As a vector for immunization, mRNA has been investigated with varying degrees of success, particularly in the field of cancer immunotherapy (76). Several factors complicate and limit the efficacy of mRNA-based therapeutics: (*i*) RNA molecules are susceptible to intracellular and extracellular degradation, (*ii*) mRNA expression is transient, and (*iii*) translational repression can occur in response to RNA (77–81). Nevertheless, administration of naked antigen-encoding mRNA can confer antitumor immunity when injected directly into lymph nodes (82, 83). Immunogenicity and/or toxicity of delivery compounds that could be used to deploy the vaccine by more amenable routes poses an additional complication. Cationic lipids, efficacious in some applications (29, 84), can be toxic when used at higher doses and if incompletely complexed (85–87). Furthermore, cationic lipids can be immunogenic, which can limit transgene expression and raise safety concerns (88). IFN production
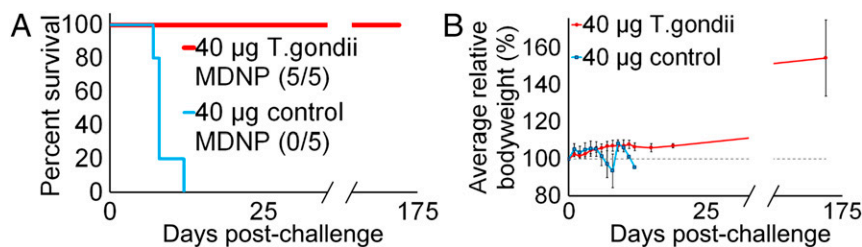
Fig. 5. VEEV-based MDNP immunization protects against lethal *T. gondii* infection. (*A*) Survival curve of animals vaccinated with hexaplex MDNPs containing GRA6, ROP2A, ROP18, SAG1, SAG2A, and AMA1 replicons. Control animals received MDNPs containing an irrelevant antigen (HA). All control animals (*n* = 5) succumbed to infection, whereas all hexaplex-immunized animals survived (*n* = 5). (*B*) Relative body weights of mice (normalized to preinfection weights) were tracked over time.

in response to lipid-complexed mRNA can limit efficacy of mRNA-based vaccines (34).

Various nanoparticle formats have demonstrated varying levels of efficacy through intradermal (89), intrasplenic (90), subcutaneous (34), intravenous (89, 91), and even intranasal (92) routes of administration. Successful applications of RNA nanoparticle-based vaccines that are independent of ex vivo transfection of antigen-presenting cells are limited in animal models (reviewed in 32, 93), and few such approaches have made it to clinical trials. Although correlates of immune protection in humans have been reported, clinical efficacy has been disappointing (94–97). Replicons based on RNA viruses of the alphavirus family, such as SFV, VEEV, and Sindbis virus (SIN), have served as vaccine vectors, usually delivered as replication-deficient pseudoviral particles generated through complementation of structural genes in cell culture (98).

Previously, PRINT protein particles were explored for the nonviral in vitro delivery of mRNA replicons (99). However, to our knowledge, only two nonviral in vivo delivery methods have been reported. These methods include a cationic nanoemulsion, comprising cationic lipid 1,2-Dioleoyl-3-trimethylammonium propane emulsified with the constituents of the MF59 adjuvant (26, 28), and a 1,2-dilinoleyloxy-3-dimethylaminopropane (DLinDMA)-centric lipid nanoparticle (27, 29), both of which are five-component systems. Although these methods have been used as a synthetic delivery method for a chimeric SIN/VEEV replicon vaccine in vivo, they have yet to show protection against lethal pathogen challenges (27–29). In contrast, our MDNP approach, a fully synthetic three-component system that uses ionizable delivery materials, lipid-anchored PEG, and replicons, confers protection in mouse models of lethal virus and protozoan infection. To our knowledge, this system is the first fully synthetic RNA-based replicon system capable of generating protective immunity against a broad variety of pathogens in lethal challenge models. This work also demonstrates that the choice of RNA payload, be it conventional mRNA or replicon, can significantly affect the intensity and persistence of antigen expression (Figs. 1*B*, 2 *A–D*, 3*A*, and 4*A*, and Fig. S2).

The MDNP delivery technology does not generate a systemic increase in inflammatory cytokine production, including IFN, when using doses 500-fold higher than the doses required for Ebola and *T. gondii* protection (49, 50), which is helpful because a strong, early IFN response may impede alphavirus replication, and thus limit the dose of antigen over time (35, 36). Furthermore, complete protection in both disease models and prolonged antigen-specific T-cell responses (at least 10 d postvaccination) were achieved in the absence of adjuvants, which are commonly used to increase the inflammatory response (13).

The lack of a systemic cytokine response to the nanoparticle delivery vehicles may also prevent antivector immunity (32). Antivector immunity occurs when the immune system responds to and inactivates the delivery vehicle, which has been observed in, for example, virus-mediated delivery platforms (100, 101). This property may also obviate the need for homologous boosting, which has

been suggested to be necessary for rVSV-based systems during recent human trials (102), which may enable repeated dosing of patients for a variety of diseases using the same delivery technology.

To respond better to evolving pathogens, sudden outbreaks, and individual patient needs, a flexible, safe, and efficient vaccine platform amenable to rapid production near the point of care is required. We believe the platform developed here has the potential to address this need by providing a synthetic system that can (*i*) allow for very rapid production following target identification; (*ii*) allow for minimal postproduction purification; (*iii*) have low potential for contaminating allergens; (*iv*) allow for relatively large payloads to permit for encapsulation of multiple antigen-producing RNAs, including replicons; (*v*) not require the use of additional adjuvants that can induce unfavorable immune responses (33), diminish endogenous mRNA production, and reduce replicon self-amplification (34–36); (*vi*) induce appropriate antibody production and CD8⁺ T-cell responses; and (*vii*) generate protective immunity with a single dose to improve patient compliance and reduce healthcare worker burden.

Materials and Methods

Cell Lines. All cells were maintained at 37 °C and 5% (vol/vol) CO_2. BHK21 cells were kindly provided by Tasuku Kitada, Weiss Laboratory, Massachusetts Institute of Technology (MIT), Cambridge, MA, and maintained in Eagle's minimal essential medium supplemented with 5% (vol/vol) FBS and 2 mM sodium pyruvate. Unless otherwise specified, BHK21 cells growing in log phase were transfected at 50–75% confluency using TransIT-mRNA transfection kits (Mirus Bio) according to the manufacturer's protocols. HeLa cells were maintained in DMEM with 10% FBS.

Mice. Wild-type female C57BL/6 and BALB/c mice were obtained from The Jackson Laboratory and used between 5 and 8 wk of age. C57BL/6 Ptprc^a mice serving as recipients of adoptive cell transfer were maintained in-house and used between 5 and 8 wk of age. OT-1/Rag1⁻/⁻ mice were maintained in-house by inbreeding of original founders purchased from Taconic. Mice were housed at the Whitehead Institute for Biomedical Research and were maintained according to protocols approved by the MIT Committee on Animal Care. A/WSN/33-infected animals were housed in an approved quarantine room at the Whitehead Institute. For Ebola studies, female C57BL/6 mice, 8–12 wk of age, were obtained from National Cancer Institute/Charles River Laboratories and housed at the US Army Medical Research Institute of Infectious Diseases (USAMRIID). Mice were vaccinated intramuscularly with the indicated MDNP at day 0 and day 21.

Plasmids and Cloning. Conventional mRNAs, without chemical modification or stabilizing UTRs, were produced by cloning the antigen of interest into the HindIII and XbaI sites in the multiple cloning site of the mammalian expression plasmid pcDNA3-EGFP (a gift from Doug Golenbock, University of Massachusetts Medical School, Worcester, MA; Addgene plasmid no. 13031) after excision of the EGFP coding sequence flanked by those restriction sequences. PCR products containing a Kozak consensus sequence (103) followed by the desired antigen coding sequence were inserted using an In-Fusion (Clontech Laboratories) cloning kit. VEEV replicon RNA vectors were produced by cloning antigens into the VEEV replicon plasmid pTK126, based on the wild-type TRD strain, kindly provided by Tasuku Kitada, Weiss Laboratory, MIT, Cambridge, MA, to replace the mVenus coding sequence that is located downstream of the VEEV subgenomic promoter sequence. Luciferase-expressing VEEV replicon pTK158 was also provided by

Tasuku Kitada. SFV replicon RNA vectors were produced by cloning antigens into a modified version of the plasmid pSFV1 (104), which was constructed by restriction digestion of pSFV1-GFP (kindly provided by Giuseppe Balistreri, Ari Helenius Laboratory, Institute of Biochemistry, Eidgenössische Technische Hochschule Zurich, Zurich, Switzerland) at the HindIII and XbaI sites, followed by ligation of the PCR fragment spanning positions 8,145–9,226 with the addition of a custom cloning site linker immediately upstream of the fragment to reconstruct the original plasmid, but carrying a unique BamHI restriction site in place of the EGFP coding sequence that was downstream of the subgenomic promoter, which served as the site of insertion for antigen coding sequences. The cOVA coding sequence was amplified by PCR from the vector pCI-neo-cOVA (64), (a gift from Maria Castro, University of California, Los Angeles; Addgene plasmid no. 25097), and was cloned into pcDNA3, pTK126, or pSFV1-JC1 using the In-Fusion cloning kit according to the manufacturer's instructions. The influenza HA coding sequence was amplified from the commercially available expression-ready influenza A H1N1 (A/WSN/33) cDNA clone, codon-optimized, full-length ORF (product no. VG11692-C; Sino Biological). EBOV GP coding sequences were amplified from pWRG7077-GP.

RNA Synthesis. RNAs for studies of luciferase and cOVA expression in tissue culture and in vivo OT-1 stimulation were generated from linearized plasmid vectors by in vitro transcription with MEGAscript kits (Life Technologies), 5′ capped to produce cap-0 structured 7-methylguanylate 5′ ends using ScriptCap m7G Capping System kits (CellScript), and 3′ poly(A)-tailed using A-Plus Poly(A) Polymerase Tailing kits (CellScript, Inc.), all according to the manufacturers' protocols. For all other experiments, replicon RNAs were synthesized essentially the same way, except for inclusion of 2′-O-methyltransferase (from ScriptCap 2′-O-methyltransferase kits; CellScript, according to the manufacturer's protocol) in the capping step to methylate the cap-adjacent 5′ nucleotide of the RNA, thus producing a cap-1 structure and ensuring more efficient first-round endogenous translation. Conventional mRNA was synthesized from the pcDNA3-derived plasmids carrying the antigen cloned into the HindIII/XbaI sites using T7 RNA polymerase after linearization with SacI. These mRNAs contained virtually no 5′ or 3′ UTR sequences, save for the short vector-derived space intervening between the T7 promoter and Kozak consensus sequence (103) at the start codon, and between the stop codon and a restriction site downstream of the SacI restriction site used for linearization. VEEV-based RNA replicon RNAs were synthesized from the vectors described above after linearization with the restriction enzyme I-SceI. I-SceI cuts downstream of the VEEV 3′ UTR and short poly(A) tract of 40 bp, and upstream of a T7 RNA polymerase promoter element preceding the VEEV 5′ UTR. SFV-based RNA replicons were constructed from the pSFV1-derived plasmids using Sp6 RNA polymerase transcription after linearization with SpeI.

Tissue Culture Protein Expression Assays. Luciferase gene expression in nanoparticle-treated cells was measured using the Steady-Glo Luciferase Assay System (Promega Corporation), according to the manufacturer's protocol. Expression of cOVA, influenza HA, and EBOV GP in RNA-transfected BHK21 cells was assayed by immunoblotting. Cells were lysed, and proteins were extracted in RIPA-benzonase buffer [20 mM Tris (pH 8), 137 mM NaCl, 0.5 mM EDTA, 10% glycerol, 1% Nonidet P-40, 0.1% SDS, 1% deoxycholate, 2 mM MgCl$_2$, 25 U/μL benzonase (EMD Millipore), and protease inhibitors (cOmplete, Mini, EDTA-free; Roche Life Science, used according to the manufacturer's recommendations)] and separated by SDS/PAGE before transfer to PVDF membranes for immunoblotting. Membranes were blocked with 10% milk in TBS-T and incubated with the following antibodies for detection in blocking buffer for 2–4 h at room temperature: for cOVA detection, rabbit polyclonal to OVA and HRP-conjugated, ab20415 (Abcam) diluted 1:3,000; for HA detection, single-chain alpaca nanobody VHH68 (70) diluted 1:1,000 followed by anti–penta-His HRP conjugate (Qiagen) diluted 1:5,000; and for EBOV GP detection, mouse monoclonal 6D8 (105) diluted 1:1,000 followed by anti-mouse HRP diluted 1:10,000. Enhanced luminol-based detection was performed using Western Lightning-ECL kits (PerkinElmer). Cell surface expression of influenza HA was assayed by dissociation of a transfected cell monolayer by trypsinization, washing once in growth medium, and staining for 15 min on ice with Alexa Fluor 647-conjugated VHH68 in PBS. Cells were washed twice with PBS, and surface staining was measured by FACS on a BD LSR II Flow Cytometer (BD Biosciences).

Modified Dendrimer Synthesis. 2-Tridecyloxirane was synthesized by the dropwise addition of 1-pentadecene (TCI) to a twofold molar excess of 3-chloroperbenzoic acid (Sigma) in dichloromethane (BDH) under constant stirring at room temperature. After reacting for 8 h, the reaction mixture was washed with equal volumes of supersaturated aqueous sodium thiosulfate solution (Sigma) three times. After each wash, the organic layer was collected using a separation funnel. Similarly, the organic layer was then washed three times

with 1 M NaOH (Sigma). Anhydrous sodium sulfate was added to the organic phase and stirred overnight to remove any remaining water. The organic layer was concentrated under vacuum to produce a slightly yellow, transparent oily liquid. This liquid was vacuum-distilled (∼6.5 Pa, ∼80 °C) to produce clear, colorless 2-tridecyloxirane. Generation 1 poly(amido amine) dendrimer with an ethylenediamine core (Dendritech) was then reacted with 2-tridecyloxirane. The stoichiometric amount of 2-tridecyloxirane was equal to 1.5-fold the total number of amine reactive sites within the dendrimer (two sites for primary amines and one site for secondary amines). Reactants were combined in cleaned 20-mL amber glass vials. Vials were filled with 200-proof ethanol as the solvent and reacted at 90 °C for 7 d in the dark under constant stirring to ensure the completion of the reaction. The crude product was mounted on a Celite 545 (VWR) precolumn and purified via flash chromatography using a CombiFlash Rf machine with a RediSep Gold Resolution silica column (Teledyne Isco) with gradient elution from 100% CH$_2$Cl$_2$ to 75:22:3 CH$_2$Cl$_2$/MeOH/NH$_4$OH$_{aq}$ (by volume) over 40 min. TLC was used to test the eluted fractions for the presence of modified dendrimers using an 87.5:11:1.5 CH$_2$Cl$_2$/MeOH/NH$_4$OH$_{aq}$ (by volume) solvent system. Modified dendrimers with different levels of substitution appeared as a distinct band on the TLC plate. Fractions containing unreacted 2-tridecyloxirane and poly(amido amine) dendrimer were discarded. Remaining fractions were combined, dried under ramping high vacuum for 12 h, and stored under a dry and inert atmosphere until used. All products contained a mixture of conformational isomers.

Nanoparticle Formulation. Nanoparticles were formulated using a microfluidic mixing device as described previously (49, 50). Briefly, modified dendrimer and 1,2-dimyristoyl-sn-glycero-3-phosphoethanolamine-N-[methoxy(polyethylene glycol)-2000] (Avanti Polar Lipids) were combined in ethanol. RNA was diluted with ultraPure, DNase/RNase-free, endotoxin-free distilled water (Invitrogen) and sterile 100 mM (pH 3.0) QB Citrate Buffer (Teknova) to a final citrate concentration of 10 mM. The ethanol and citrate streams were loaded into gas-tight glass syringes (Hamilton), and using a microfluidic mixing device, the ethanol and citrate streams were combined and mixed in a 1:3 volumetric flow rate ratio (combined total flow rate equal to 5.3 mL/min) to produce nanoparticles. Using glassware washed for 24 h in 1.0 M NaOH (Sigma) for endotoxin removal and sterilized in a steam autoclave, nanoparticles were dialyzed against sterile, endotoxin-free PBS using 20,000 molecular weight cut-off Slide-A-Lyzer G2 dialysis cassettes. Dialyzed nanoparticles were sterile-filtered using 0.2 μm poly(ether sulfone) filters (Genesee Scientific) and characterized with a Zetasizer NanoZS machine (Malvern). The concentration of RNA was determined by theoretical mass balance calculations and confirmed by Nano-Drop measurement (Thermo Scientific). The final nanoparticles contained an 11.5:1:2.3 mass ratio of modified dendrimer to 1,2-dimyristoyl-sn-glycero-3-phosphoethanolamine-N-[methoxy(polyethylene glycol)-2000] to RNA.

Real-Time Analysis of Nanoparticle Disassembly. FRET was used to estimate the stability of nanoparticles under simulated intramuscular conditions. Desalted, HPLC-purified RNA duplexes labeled at the 5′ end of the sense strand with either Alexa Fluor 594 or Alexa Fluor 647 dye were purchased from Integrated DNA Technologies. Nanoparticles with equimolar amounts of both types of RNA were formulated and diluted to a final RNA concentration of 2 μg/mL. In quadruplets, 100 μL of the diluted nanoparticles was added to each well of an opaque black 96-well plate. One hundred microliters of 50% AB human serum (Invitrogen), which had been diluted in PBS, was added to each well. Negative control wells contained free siRNA. Positive control wells contained polyethylenimine (PEI) nanoparticles. PEI nanoparticles were formed by the repeat pipetting of 800 MW PEI (Sigma) with RNA in a 5:1 PEI-to-RNA mass ratio in a 10 wt% sucrose solution. The plate was sealed with a clear adhesive plate seal and placed into a Tecan Infinite M200 microplate reader set to 37 °C. To measure FRET, samples were excited at 540 nm and the fluorescent intensity was read at 690 nm and 620 nm every 5 min for 2 h. FRET was calculated as the 690-nm/620-nm fluorescent intensity signal ratio. FRET values were normalized to the values of the completely ruptured nanoparticle, which were determined after adding octyl β-D-glucopyranoside (Sigma) to a final in-well concentration of 2 wt% and mixing for 1 h at 37 °C.

In Vivo Experiments. All animal studies were approved by the MIT, Whitehead Institute, and USAMRIID Institutional Animal Care and Use Committees and were also consistent with all applicable local, state, and federal regulations.

Adoptive Transfer and OT-1 Proliferation Assays. OT-1 cells were isolated from the mesenteric and inguinal lymph nodes and spleens of transgenic 6- to 12-wk-old OT-1/Rag1$^{-/-}$ C57BL/6 mice and resuspended in PBS. The cells were labeled for 5 min at room temperature with CFSE (Sigma) at a final concentration of 5 μM, and then washed once in RPMI supplemented with 10% FBS before

resuspension in PBS for injection. Wild-type CD45.1 mice at 4–8 wk of age received 1.5 million labeled OT-1 cells by i.v. injection. Four days after adoptive transfer, inguinal lymph nodes were dissected and lymphocytes were isolated for FACS analysis. Cells were stained with 7-AAD (BD Biosciences), Alexa Fluor 700- or APC-conjugated anti-CD45.1, phycoerythrin (PE)-Cy7– or APC-Cy7–conjugated anti-CD45.2, and Pacific Blue- or PE-conjugated anti-CD8. Stained samples were analyzed by FACS on a BD LSR II Flow Cytometer (BD Biosciences).

T-Cell Activation Assay. Splenocytes were isolated from mice and plated at a density of 10 million cells per milliliter in 96-well culture plates in the presence of growth medium [all components were from Life Technologies unless otherwise indicated: RPMI 1620 with GlutaMAX supplemented with 8% FBS, 1 mM nonessential amino acids, 1 mM sodium pyruvate, 10 mM Hepes, 50 μM 2-mercaptoethanol (Sigma), and penicillin/streptomycin] only or 2 μg/mL OVA-derived peptide in growth medium. Peptides used were the immunodominant H-2K^b–restricted MHC class I OVA-derived peptide SIINFEKL (InvivoGen) or the H-2 I-A^b MHC class II-restricted peptide ISQAVHAAHAEINEAGR (InvivoGen). After 5 d in culture, the concentration of 1:20 diluted supernatant IFN-γ was quantified using IFN-γ ELISA kits (BD Biosciences).

Anti-HA IgG ELISA. High-binding, surface-treated, polystyrene 96-well microplates (Corning) were coated overnight at 4 °C with 0.5 μg/mL recombinant influenza A H1N1 WSN/33 protein (Sino Biological, Inc.) in PBS. Plates were blocked for 2 h with blocking buffer (PBS with 10% FBS) at room temperature, serum was applied to wells in duplicate at a 1:100 dilution in blocking buffer, and wells were incubated for 2 h at room temperature. Plates were washed with wash buffer (PBS with 0.05% Tween-20) and incubated at room temperature with anti-mouse IgG-HRP (GE Healthcare) diluted 1:3,000 in blocking buffer for 1 h. After five rounds of washing with wash buffer, plates were developed with TMB substrate (Sigma) for 20–30 min, and the reaction was stopped by the addition of 1 vol of 1 M HCl before reading absorbance at 450 nm.

T-Cell Intracellular Cytokine Staining Assay. Splenocytes were isolated from mice 9 d after immunization with 40 μg MDNP and cultured in growth medium [all components were from Life Technologies unless otherwise indicated: RPMI 1620 with GlutaMAX supplemented with 8% FBS, 1 mM nonessential amino acids, 1 mM sodium pyruvate, 10 mM Hepes, 50 μM 2-mercaptoethanol (Sigma), and penicillin/streptomycin]. Cytokine expression in response to stimulation with the immunodominant H-2K^b–restricted MHC class I OVA-derived peptide SIINFEKL (InvivoGen) or EBOV GP-derived WE15 peptide (WIPYFGPAAEGIYTE) was assayed by intracellular cytokine staining and FACS analysis essentially as described previously (71). Briefly, 1×10^7 splenocytes per milliliter were cultured in the presence of IL-2 (10 U/mL), anti-CD28 + anti-CD49d (0.5 μg/mL each; BioLegend), and Brefeldin A (2 μg/mL final; Sigma) with or without 2 μg/mL peptide. The IL-2, anti-CD28, and anti-CD49d were omitted for stimulation with SIINFEKL, because the splenic response to this peptide in OVA-vaccinated mice is apparent even without exogenous costimulation. Cultures stimulated nonspecifically with 0.1 μg/mL PMA and 1 μg/mL ionomycin were used as single-color antibody staining controls for FACS analysis. After 6 h in culture, cells were stained using a BD Cytofix/Cytoperm kit (BD Biosciences) according to the manufacturer's protocol with FITC-conjugated anti-CD8 (BioLegend), APC-conjugated anti-CD4 (BioLegend), PE-conjugated anti–IFN-γ (BD Biosciences), and Pacific Blue-conjugated IL-2 (BioLegend). Stained samples were analyzed by FACS on a BD LSR II Flow Cytometer (BD Biosciences).

Influenza Challenge. Immunized mice were inoculated by intranasal administration of a lethal dose [5×10^4 chicken embryo infectious dose 50% (CEID$_{50}$)] of influenza A/NWS/33 (H1N1; American Type Culture Collection), which, in our hands, kills 100% of infected BALB/c mice in under 9 d. Body weight was monitored daily, and mice were euthanized when over 20% loss was observed. Mice were considered recovered when preinfection body weight was surpassed, and their health was monitored for an additional 3 wk to ensure no clinical signs of infection were observed.

EBOV GP Serum ELISA. Blood was collected at the indicated time points in serum separation tubes. ELISA plates were coated at 4 °C overnight with recombinant mammalian Ebola GP at 2 μg/mL in PBS. Plates were washed three times with PBS plus 0.1% Tween-20 (PBS-T) and then blocked for 2 h at room temperature with PBS-T 5% nonfat milk. Serum was diluted by half-log dilutions starting at 1:100 and incubated for 1 h on GP-coated plates. Plates were then washed three times with PBS-T, incubated with the indicated secondary HRP-antibody for 45 min, and then washed three times with PBS-T. ELISA was developed using TMB substrate/stop solution and measured on a Tecan plate reader. Absorbance cutoff was determined as background + 0.2 OD.

EBOV Challenge. Mice were inoculated with a target titer of 1,000 pfu of ma-EBOV (72). All studies were conducted in the USAMRIID Biosafety Level 4 containment facility. Beginning on day 0 and continuing for the duration of the in-life phase, clinical observations were recorded and animals were closely monitored for disease progression. Moribund animals were euthanized based on institutionally approved clinical scoring.

T. gondii Challenge. The wild-type PRU-delta HXGPRT strain of _T. gondii_ parasites, a gift from the Jeroen J. P. Saeij laboratory, University of California, Davis, CA, were prepared as previously described (106). Mice were inoculated with 10^5 tachyzoites. Animals were monitored for clinical signs of sickness, including weight loss, poor grooming, lethargy, squinting, dehydration, and drops in body temperature. Mice were euthanized if they experienced over 10% weight loss, severe dehydration, severe lethargy, or significant drops in body temperature.

Electrospray Ionization. Electrospray ionization analysis of the modified dendrimer nanomaterial was performed as a service provided by the Swanson Biotechnology Center at MIT.

Statistical Analysis. Means were compared by ANOVA with Tukey multiple comparison corrections. For survival curves, the Mantel–Cox test was used. P values below 0.05 were considered statistically significant.

1. Arnon R, Ben-Yedidia T (2003) Old and new vaccine approaches. _Int Immunopharmacol_ 3(8):1195–1204.
2. Azad N, Rojanasakul Y (2006) Vaccine delivery—Current trends and future. _Curr Drug Deliv_ 3(2):137–146.
3. Koblin BA, et al.; NIAID HIV Vaccine Trials Network (2011) Safety and immunogenicity of an HIV adenoviral vector boost after DNA plasmid vaccine prime by route of administration: A randomized clinical trial. _PLoS One_ 6(9):e24517.
4. Pittman PR (2002) Aluminum-containing vaccine associated adverse events: Role of route of administration and gender. _Vaccine_ 20(Suppl 3):S48–S50.
5. Scheiermann J, Klinman DM (2014) Clinical evaluation of CpG oligonucleotides as adjuvants for vaccines targeting infectious diseases and cancer. _Vaccine_ 32(48):6377–6389.
6. Aucouturier J, Ascarateil S, Dupuis L (2006) The use of oil adjuvants in therapeutic vaccines. _Vaccine_ 24(Suppl 2):44–45.
7. Mulligan MJ, et al.; DMID 13-0032 H7N9 Vaccine Study Group (2014) Serological responses to an avian influenza A/H7N9 vaccine mixed at the point-of-use with MF59 adjuvant: A randomized clinical trial. _JAMA_ 312(14):1409–1419.
8. Cox RJ, et al. (2011) Evaluation of a virosomal H5N1 vaccine formulated with Matrix M™ adjuvant in a phase I clinical trial. _Vaccine_ 29(45):8049–8059.
9. Mata E, Salvador A, Igartua M, Hernández RM, Pedraz JL (2013) Malaria vaccine adjuvants: Latest update and challenges in preclinical and clinical research. _BioMed Res Int_ 2013:282913.
10. Rizza P, Capone I, Moretti F, Proietti E, Belardelli F (2011) IFN-α as a vaccine adjuvant: Recent insights into the mechanisms and perspectives for its clinical use. _Expert Rev Vaccines_ 10(4):487–498.
11. Stephenson R, You H, McManus DP, Toth I (2014) Schistosome vaccine adjuvants in preclinical and clinical research. _Vaccines (Basel)_ 2(3):654–685.
12. Innes EA, Bartley PM, Maley S, Katzer F, Buxton D (2009) Veterinary vaccines against _Toxoplasma gondii_. _Mem Inst Oswaldo Cruz_ 104(2):246–251.
13. Schijns VE, Lavelle EC (2011) Trends in vaccine adjuvants. _Expert Rev Vaccines_ 10(4):539–550.
14. Plotkin SA, Orenstein WA, Offit PA (2012) _Vaccines_ (Elsevier, Amsterdam), 6th Ed.
15. Rappuoli R, Pizza M, Del Giudice G, De Gregorio E (2014) Vaccines, new opportunities for a new society. _Proc Natl Acad Sci USA_ 111(34):12288–12293.
16. Rock KL, Goldberg AL (1999) Degradation of cell proteins and the generation of MHC class I-presented peptides. _Annu Rev Immunol_ 17:739–779.
17. Lauring AS, Jones JO, Andino R (2010) Rationalizing the development of live attenuated virus vaccines. _Nat Biotechnol_ 28(6):573–579.
18. MacGregor RR, et al. (1998) First human trial of a DNA-based vaccine for treatment of human immunodeficiency virus type 1 infection: Safety and host response. _J Infect Dis_ 178(1):92–100.
19. Tang DC, DeVit M, Johnston SA (1992) Genetic immunization is a simple method for eliciting an immune response. _Nature_ 356(6365):152–154.

20. Fynan EF, et al. (1993) DNA vaccines: Protective immunizations by parenteral, mucosal, and gene-gun inoculations. *Proc Natl Acad Sci USA* 90(24):11478–11482.

21. Bagarazzi ML, et al. (2012) Immunotherapy against HPV16/18 generates potent TH1 and cytotoxic cellular immune responses. *Sci Transl Med* 4(155):155ra138.

22. Ferraro B, et al. (2011) Clinical applications of DNA vaccines: Current progress. *Clin Infect Dis* 53(3):296–302.

23. Wang Z, et al. (2004) Detection of integration of plasmid DNA into host genomic DNA following intramuscular injection and electroporation. *Gene Ther* 11(8):711–721.

24. Petsch B, et al. (2012) Protective efficacy of in vitro synthesized, specific mRNA vaccines against influenza A virus infection. *Nat Biotechnol* 30(12):1210–1216.

25. Kallen K-J, et al. (2013) A novel, disruptive vaccination technology: Self-adjuvanted RNActive(®) vaccines. *Hum Vaccin Immunother* 9(10):2263–2276.

26. Brito LA, et al. (2014) A cationic nanoemulsion for the delivery of next-generation RNA vaccines. *Mol Ther* 22(12):2118–2129.

27. Hekele A, et al. (2013) Rapidly produced SAM(®) vaccine against H7N9 influenza is immunogenic in mice. *Emerg Microbes Infect* 2(8):e52.

28. Bogers WM, et al. (2015) Potent immune responses in rhesus macaques induced by nonviral delivery of a self-amplifying RNA vaccine expressing HIV type 1 envelope with a cationic nanoemulsion. *J Infect Dis* 211(6):947–955.

29. Geall AJ, et al. (2012) Nonviral delivery of self-amplifying RNA vaccines. *Proc Natl Acad Sci USA* 109(36):14604–14609.

30. Perri S, et al. (2003) An alphavirus replicon particle chimera derived from venezuelan equine encephalitis and sindbis viruses is a potent gene-based vaccine delivery vector. *J Virol* 77(19):10394–10403.

31. Ljungberg K, Liljeström P (2015) Self-replicating alphavirus RNA vaccines. *Expert Rev Vaccines* 14(2):177–194.

32. Ulmer JB, Mason PW, Geall A, Mandl CW (2012) RNA-based vaccines. *Vaccine* 30(30):4414–4418.

33. Gupta RK, et al. (1993) Adjuvants–a balance between toxicity and adjuvanticity. *Vaccine* 11(3):293–306.

34. Pollard C, et al. (2013) Type I IFN counteracts the induction of antigen-specific immune responses by lipid-based delivery of mRNA vaccines. *Mol Ther* 21(1):251–259.

35. White LJ, Wang JG, Davis NL, Johnston RE (2001) Role of alpha/beta interferon in Venezuelan equine encephalitis virus pathogenesis: Effect of an attenuating mutation in the 5′ untranslated region. *J Virol* 75(8):3706–3718.

36. Zhang Y, Burke CW, Ryman KD, Klimstra WB (2007) Identification and characterization of interferon-induced proteins that inhibit alphavirus replication. *J Virol* 81(20):11246–11255.

37. D'Alessio G (2011) The superfamily of vertebrate-secreted ribonucleases. *Ribonucleases, Nucleic Acids and Molecular Biology*, ed Nicholson AW (Springer, Heidelberg), pp 1–34.

38. Thess A, et al. (2015) Sequence-engineered mRNA without chemical nucleoside modifications enables an effective protein therapy in large animals. *Mol Ther* 23(9):1456–1464.

39. Kariko K, Muramatsu H, Keller JM, Weissman D (2012) Increased erythropoiesis in mice injected with submicrogram quantities of pseudouridine-containing mRNA encoding erythropoietin. *Mol Ther* 20(5):948–953.

40. Wang Z, Tiruppathi C, Minshall RD, Malik AB (2009) Size and dynamics of caveolae studied using nanoparticles in living endothelial cells. *ACS Nano* 3(12):4110–4116.

41. Maeda H, Fang J, Inutsuka T, Kitamoto Y (2003) Vascular permeability enhancement in solid tumor: Various factors, mechanisms involved and its implications. *Int Immunopharmacol* 3(3):319–328.

42. Schwartz S, et al. (2014) Transcriptome-wide mapping reveals widespread dynamic-regulated pseudouridylation of ncRNA and mRNA. *Cell* 159(1):148–162.

43. Ganot P, Bortolin ML, Kiss T (1997) Site-specific pseudouridine formation in preribosomal RNA is guided by small nucleolar RNAs. *Cell* 89(5):799–809.

44. Cantara WA, et al. (2011) The RNA Modification Database, RNAMDB: 2011 update. *Nucleic Acids Res* 39(Database issue):D195–D201.

45. Helm M (2006) Post-transcriptional nucleotide modification and alternative folding of RNA. *Nucleic Acids Res* 34(2):721–733.

46. Yin H, et al. (2014) Non-viral vectors for gene-based therapy. *Nat Rev Genet* 15(8):541–555.

47. Whitehead KA, et al. (2014) Degradable lipid nanoparticles with predictable in vivo siRNA delivery activity. *Nat Commun* 5:4277.

48. Wan C, Allen TM, Cullis PR (2014) Lipid nanoparticle delivery systems for siRNA-based therapeutics. *Drug Deliv Transl Res* 4(1):74–83.

49. Khan OF, et al. (2014) Ionizable amphiphilic dendrimer-based nanomaterials with alkyl-chain-substituted amines for tunable siRNA delivery to the liver endothelium in vivo. *Angew Chem Int Ed Engl* 53(52):14397–14401.

50. Khan OF, et al. (2015) Dendrimer-inspired nanomaterials for the in vivo delivery of siRNA to lung vasculature. *Nano Lett* 15(5):3008–3016.

51. Duncan R, Ringsdorf H, Satchi-Fainaro R (2006) Polymer therapeutics: Polymers as drugs, drug and protein conjugates and gene delivery systems: Past, present and future opportunities. *Polymer Therapeutics I, Advances in Polymer Science*, eds Satchi-Fainaro R, Duncan R (Springer, Berlin), Vol 192, pp 1–8.

52. National Institute of Allergy and Infectious Diseases (2015) NIAID Emerging Infectious Diseases/Pathogens. Available at https://www.niaid.nih.gov/topics/biodefenserelated/biodefense/pages/cata.aspx. Accessed June 14, 2016.

53. Partridge J, Kieny MP; World Health Organization H1N1 influenza vaccine Task Force (2010) Global production of seasonal and pandemic (H1N1) influenza vaccines in 2009-2010 and comparison with previous estimates and global action plan targets. *Vaccine* 28(30):4709–4712.

54. Gerdil C (2003) The annual production cycle for influenza vaccine. *Vaccine* 21(16):1776–1779.

55. Kilbourne ED, et al. (1971) Related studies of a recombinant influenza-virus vaccine. I. Derivation and characterization of virus and vaccine. *J Infect Dis* 124(5):449–462.

56. Chen Z, et al. (2010) Generation of live attenuated novel influenza virus A/California/7/09 (H1N1) vaccines with high yield in embryonated chicken eggs. *J Virol* 84(1):44–51.

57. Biesova Z, et al. (2009) Preparation, characterization, and immunogenicity in mice of a recombinant influenza H5 hemagglutinin vaccine against the avian H5N1 A/Vietnam/1203/2004 influenza virus. *Vaccine* 27(44):6234–6238.

58. Wurm FM (2004) Production of recombinant protein therapeutics in cultivated mammalian cells. *Nat Biotechnol* 22(11):1393–1398.

59. Chu L, Robinson DK (2001) Industrial choices for protein production by large-scale cell culture. *Curr Opin Biotechnol* 12(2):180–187.

60. Li M, Qiu YX (2013) A review on current downstream bio-processing technology of vaccine products. *Vaccine* 31(9):1264–1267.

61. Lua LH, et al. (2014) Bioengineering virus-like particles as vaccines. *Biotechnol Bioeng* 111(3):425–440.

62. Boussif O, et al. (1995) A versatile vector for gene and oligonucleotide transfer into cells in culture and in vivo: Polyethylenimine. *Proc Natl Acad Sci USA* 92(16):7297–7301.

63. Brito LA, Singh M (2011) Acceptable levels of endotoxin in vaccine formulations during preclinical research. *J Pharm Sci* 100(1):34–37.

64. Yang J, et al. (2010) Kupfer-type immunological synapse characteristics do not predict anti-brain tumor cytolytic T-cell function in vivo. *Proc Natl Acad Sci USA* 107(10):4716–4721.

65. Rötzschke O, et al. (1991) Exact prediction of a natural T cell epitope. *Eur J Immunol* 21(11):2891–2894.

66. Leitner WW, et al. (2003) Alphavirus-based DNA vaccine breaks immunological tolerance by activating innate antiviral pathways. *Nat Med* 9(1):33–39.

67. Leitner WW, Bergmann-Leitner ES, Hwang LN, Restifo NP (2006) Type I Interferons are essential for the efficacy of replicase-based DNA vaccines. *Vaccine* 24(24):5110–5118.

68. Levine B, et al. (1993) Conversion of lytic to persistent alphavirus infection by the bcl-2 cellular oncogene. *Nature* 361(6414):739–742.

69. Ying H, et al. (1999) Cancer therapy using a self-replicating RNA vaccine. *Nat Med* 5(7):823–827.

70. Dougan SK, et al. (2013) Antigen-specific B-cell receptor sensitizes B cells to infection by influenza virus. *Nature* 503(7476):406–409.

71. Martins KA, et al. (2014) Toll-like receptor agonist augments virus-like particle-mediated protection from Ebola virus with transient immune activation. *PLoS One* 9(2):e89735.

72. Kuhn JH, et al. (2013) Virus nomenclature below the species level: A standardized nomenclature for laboratory animal-adapted strains and variants of viruses assigned to the family Filoviridae. *Arch Virol* 158(6):1425–1432.

73. Zhang NZ, Chen J, Wang M, Petersen E, Zhu XQ (2013) Vaccines against Toxoplasma gondii: New developments and perspectives. *Expert Rev Vaccines* 12(11):1287–1299.

74. Hoffmann S, Batz MB, Morris JG, Jr (2012) Annual cost of illness and quality-adjusted life year losses in the United States due to 14 foodborne pathogens. *J Food Prot* 75(7):1292–1302.

75. Srivastava IK, Liu MA (2003) Gene vaccines. *Ann Intern Med* 138(7):550–559.

76. Van Lint S, et al. (2015) The ReNAissanCe of mRNA-based cancer therapy. *Expert Rev Vaccines* 14(2):235–251.

77. Baum A, García-Sastre A (2010) Induction of type I interferon by RNA viruses: Cellular receptors and their substrates. *Amino Acids* 38(5):1283–1299.

78. Heil F, et al. (2004) Species-specific recognition of single-stranded RNA via toll-like receptor 7 and 8. *Science* 303(5663):1526–1529.

79. Karikó K, Ni H, Capodici J, Lamphier M, Weissman D (2004) mRNA is an endogenous ligand for Toll-like receptor 3. *J Biol Chem* 279(13):12542–12550.

80. Pichlmair A, et al. (2006) RIG-I-mediated antiviral responses to single-stranded RNA bearing 5′-phosphates. *Science* 314(5801):997–1001.

81. Levin DH, Petryshyn R, London IM (1981) Characterization of purified double-stranded RNA-activated eIF-2 alpha kinase from rabbit reticulocytes. *J Biol Chem* 256(14):7638–7641.

82. Kreiter S, et al. (2010) Intranodal vaccination with naked antigen-encoding RNA elicits potent prophylactic and therapeutic antitumoral immunity. *Cancer Res* 70(22):9031–9040.

83. Van Lint S, et al. (2012) Preclinical evaluation of TriMix and antigen mRNA-based antitumor therapy. *Cancer Res* 72(7):1661–1671.

84. Bogers WM, et al. (2014) Potent immune responses in rhesus macaques induced by nonviral delivery of a self-amplifying RNA vaccine expressing HIV type 1 envelope with a cationic nanoemulsion. *J Infect Dis* 211(6):947–955.

85. Hofland HE, Shephard L, Sullivan SM (1996) Formation of stable cationic lipid/DNA complexes for gene transfer. *Proc Natl Acad Sci USA* 93(14):7305–7309.

86. Cullis PR, Chonn A, Semple SC (1998) Interactions of liposomes and lipid-based carrier systems with blood proteins: Relation to clearance behaviour in vivo. *Adv Drug Deliv Rev* 32(1-2):3–17.

87. Lv H, Zhang S, Wang B, Cui S, Yan J (2006) Toxicity of cationic lipids and cationic polymers in gene delivery. *J Control Release* 114(1):100–109.

88. Henriksen-Lacey M, et al. (2011) Comparison of the depot effect and immunogenicity of liposomes based on dimethyldioctadecylammonium (DDA), 3β-[N-(N′,N′-Dimethylaminoethane)carbomyl] cholesterol (DC-Chol), and 1,2-Dioleoyl-3-trimethylammonium propane (DOTAP): Prolonged liposome retention mediates stronger Th1 responses. *Mol Pharm* 8(1):153–161.

89. Hoerr I, Obst R, Rammensee HG, Jung G (2000) In vivo application of RNA leads to induction of specific cytotoxic T lymphocytes and antibodies. *Eur J Immunol* 30(1):1–7.

90. Zhou WZ, et al. (1999) RNA melanoma vaccine: Induction of antitumor immunity by human glycoprotein 100 mRNA immunization. *Hum Gene Ther* 10(16):2719–2724.

91. Mockey M, et al. (2007) mRNA-based cancer vaccine: Prevention of B16 melanoma progression and metastasis by systemic injection of MART1 mRNA histidylated lipopolyplexes. *Cancer Gene Ther* 14(9):802–814.

92. Phua KK, Staats HF, Leong KW, Nair SK (2014) Intranasal mRNA nanoparticle vaccination induces prophylactic and therapeutic anti-tumor immunity. *Sci Rep* 4:5128.

93. Weiner DB (2013) RNA-based vaccination: Sending a strong message. *Mol Ther* 21(3):506–508.

94. Weide B, et al. (2008) Results of the first phase I/II clinical vaccination trial with direct injection of mRNA. *J Immunother* 31(2):180–188.

95. Weide B, et al. (2009) Direct injection of protamine-protected mRNA: Results of a phase 1/2 vaccination trial in metastatic melanoma patients. *J Immunother* 32(5):498–507.

96. Rittig SM, et al. (2011) Intradermal vaccinations with RNA coding for TAA generate CD8+ and CD4+ immune responses and induce clinical benefit in vaccinated patients. *Mol Ther* 19(5):990–999.

97. Kreiter S, Diken M, Selmi A, Türeci Ö, Sahin U (2011) Tumor vaccination using messenger RNA: Prospects of a future therapy. *Curr Opin Immunol* 23(3):399–406.

98. Lundstrom K (2015) Alphaviruses in gene therapy. *Viruses* 7(5):2321–2333.

99. Xu J, et al. (2013) RNA replicon delivery via lipid-complexed PRINT protein particles. *Mol Pharm* 10(9):3366–3374.

100. Small JC, Ertl HCJ (2011) Viruses—From pathogens to vaccine carriers. *Curr Opin Virol* 1(4):241–245.

101. Lopez-Gordo E, Podgorski II, Downes N, Alemany R (2014) Circumventing antivector immunity: Potential use of nonhuman adenoviral vectors. *Hum Gene Ther* 25(4):285–300.

102. Fuchs JD, et al.; HVTN 090 Study Group and the National Institutes of Allergy and Infectious Diseases HIV Vaccine Trials Network (2015) First-in-human evaluation of the safety and immunogenicity of a recombinant vesicular stomatitis virus human immunodeficiency virus-1 gag vaccine (HVTN 090). *Open Forum Infect Dis* 2(3):ofv082.

103. Kozak M (1987) An analysis of 5′-noncoding sequences from 699 vertebrate messenger RNAs. *Nucleic Acids Res* 15(20):8125–8148.

104. Liljeström P, Garoff H (1991) A new generation of animal cell expression vectors based on the Semliki Forest virus replicon. *Biotechnology (N Y)* 9(12):1356–1361.

105. Wilson JA, et al. (2000) Epitopes involved in antibody-mediated protection from Ebola virus. *Science* 287(5458):1664–1666.

106. Sidik SM, Hackett CG, Tran F, Westwood NJ, Lourido S (2014) Efficient genome engineering of *Toxoplasma gondii* using CRISPR/Cas9. *PLoS One* 9(6):e100450.